Weather and Climate Extremes 5-6 (2014) 16–28

Contents lists available at ScienceDirect

Weather and Climate Extremes

journal homepage: www.elsevier.com/locate/wace

The 19 January 2013 windstorm over the North Atlantic: large-scale dynamics and impacts on Iberia

Margarida L.R. Liberato [a,b,*]

[a] Escola de Ciências e Tecnologia, Universidade de Trás-os-Montes e Alto Douro, UTAD, Vila Real, Portugal
[b] Instituto Dom Luiz (IDL), Faculdade de Ciências, Universidade de Lisboa, Lisboa, Portugal

ARTICLE INFO

Article history:
Received 31 December 2013
Received in revised form
13 June 2014
Accepted 29 June 2014
Available online 17 July 2014

Keywords:
Explosive cyclogenesis
Atmospheric river
Windstorm
Iberia
Wind and precipitation extremes
Natural hazards

ABSTRACT

On 19 January 2013 Portugal was once again on an extreme meteorological risk warning state due to the landfall of a rapidly deepening low pressure system exactly on the period of its maximum explosive development. This storm, named Gong, had a central minimum pressure of 968 hPa, observed wind gusts of 140 km h^{-1} on some locations of the Portuguese coast and was responsible for the downfall of thousands of trees on some of the Portuguese national forests, the destruction of several hundred farms among other huge socioeconomic losses and fatalities.

The large-scale synoptic conditions and dynamical characteristics of windstorm Gong, as well as the associated meteorological and socioeconomic adverse impacts are reviewed in this paper. For this purpose an objective lagrangean method, which identifies and follows individual lows, is applied for the assessment of the cyclone track and lifetime characteristics, which is complemented by the analysis of several thermohydrodynamical reanalysis fields during the lifetime of the cyclone.

Results show that Gong underwent an explosive development with 'bomb' characteristics between the Azores and the Iberian Peninsula, with a deepening rate unusually high for these latitudes. The rapid deepening of Gong was supported by the southerly displacement of the polar jet stream; by a pronounced cyclonic potential vorticity streamer which approached Iberia from northwest; and by the presence of an atmospheric river over the western and central subtropical North Atlantic converging into Gong's genesis region and then crossing the Atlantic basin, moving along with the storm towards Iberia. Understanding the dynamics of these high impact extreme events may be of relevance in view of improving extreme forecasts as well as of public awareness, policy making and risk assessment and management of severe weather in Portugal.

1. Introduction

Extreme windstorms are one of the major natural catastrophes in the extratropics, one of the most costly natural hazards in Europe and are responsible for substantial economic damages and even fatalities. During the last decades Europe witnessed major damage from winter storms such as Lothar (December 1999), Kyrill (January 2007), Klaus (January 2009) and Xynthia (February 2010) which exhibited uncommon characteristics. In fact, both Klaus and Xynthia crossed the Atlantic in direction of Europe experiencing an explosive development at unusual lower latitudes along the edge of the dominant North Atlantic storm track and reaching Iberia with an uncommon intensity (Liberato et al., 2011, 2013). On the other hand, storm Kyrill reached Eastern Europe with an uncommon intensity (Fink et al., 2009). The storm names employed herein are as given by the Institute of Meteorology of the Freie Universität Berlin and as used by the German Weather Service (Source: http://www.met.fu-berlin.de/adopt-a-vortex/historie/).

In recent years several authors have focused their research on the inter-comparison of storm-tracks derived from different reanalysis datasets, including improved resolution of the models and improved assimilation schemes (e.g. Schmith et al., 1998; Ulbrich and Christoph, 1999; Sickmöller et al., 2000; Trigo, 2006; Raible et al., 2008; Hodges et al., 2011). On the North Atlantic, Trigo (2006) showed two zonal bands, one exhibiting an overall increase of storms, ranging from the Labrador Sea to Scandinavia, and a second band, dominated by decreasing cyclone counts, which ranges from the Azores to Central Europe and the Mediterranean. Many papers support a northward and eastward shift in the Atlantic cyclone activity during the last six decades with both more frequent and more intense wintertime cyclones in the high-latitude Atlantic

* Correspondence address: Universidade de Trás-os-Montes e Alto Douro, UTAD, Quinta de Prados, Apartado 1013, 5000-801 Vila Real, Portugal.
Tel.: +351 259 350 319; fax: +351 259 350 356.
E-mail address: mlr@utad.pt

http://dx.doi.org/10.1016/j.wace.2014.06.002

(Schneidereit et al., 2007; Raible et al., 2008; Vilibic and Sepic, 2010) and fewer in the mid-latitude Atlantic (Wang et al., 2006; Raible et al., 2008). This pattern, suggesting a northward shift of storm-tracks has been associated with the fluctuations observed during the last decades of the main mode of atmospheric variability in the Euro-Atlantic sector - the North Atlantic Oscillation (Trigo, 2006; Pinto et al., 2011). Furthermore Donat et al. (2011) and Wang et al. (2012) found significant increases in both the strength and frequency of wintertime storms for large parts of Europe using the 20th century Reanalysis (Compo et al., 2011).

However, comparisons between studies depend both on the sensitivities in identification schemes and on different definitions for extreme cyclones (Ulbrich et al., 2009; Neu et al., 2013). Neu et al. (2013) compared different cyclone identification and tracking algorithms for the research over the same ERA Interim reanalysis dataset. While absolute numbers of detected cyclones show large spreads between the methods, trends of track densities are well captured across the algorithms. In addition, major climate change signals seem to be robust, independent of the method used (Ulbrich et al., 2013). In fact, Ulbrich et al. (2013) showed that increases in cyclone track densities are consistently found in the eastern North Atlantic west of the British Isles, with changes between 3% and 9%, whereas only one method showed a decrease of cyclones. This paper made evidence that the change in this region is highly influenced by strong cyclones which are consistently tracked by the different methods. For strong cyclones, the changes in the North Atlantic box range from about 20% to 35%.

Under this context, though the occurrence of recent storms like Klaus (January 2009) and Xynthia (February 2010) may be considered to be part of the climate system's natural variability, the fact is that such rare event occurred once again in the winter of 2013 near the coast of Iberia. It is worth noting that historical studies on windstorms affecting Portugal register only very rare events, such as the ones occurring in February 1941 (Muir-Wood, 2011; Freitas and Dias, 2013) and in November 1724, which was one of the most destructive storms ever experienced in Portugal since the early 17th century (Domínguez-Castro et al., 2013). Gong is another extreme windstorm, with the explosive development occurring at unusual lower latitudes, heading towards Iberia and being responsible for considerable high socioeconomic impacts over Portugal. Analysing and understanding the dynamical mechanisms that favour the development and unusual intensification of this storm near Iberia and the identification of the associated meteorological and socioeconomic adverse impacts may be of relevance in view of increasing public awareness for other similar disasters, enhancing policy makers' awareness on the necessity of concrete measures to mitigate their effects and motivating risk assessment and management of severe weather in Portugal. For all these reasons it deserves being studied here in detail.

In this paper we present a thorough assessment of windstorm Gong (18–19 January 2013). The paper is organized as follows. Section 2 contains a description of the data and methods used. A brief overview of the cyclone lifecycle, with special emphasis on its explosive development on the Eastern North Atlantic, near Iberia is presented in Section 3. In Section 4 the synoptic description of the large-scale atmospheric conditions prior to and during the explosive development of Gong as well as the influence of the atmospheric river on its cyclogenesis and intensification are presented. The storm's meteorological and socioeconomic impacts over Portugal are also briefly described in Section 5 while implications and conclusions are presented in the final section.

2. Data and methodology

The European Centre for Medium-Range Weather Forecasts (ECMWF) Reanalysis (ERA Interim; Dee et al., 2011) namely, the geopotential height fields, wind, divergence data, temperature and the relative and specific humidity at 27 pressure levels (from 100 to 1000 hPa), the mean sea level pressure (MSLP) and total column water vapour (TCWV) have been used for the Euro-Atlantic region (85°W–20°E; 10°N–60°N). These fields were extracted for January 2013 at full temporal (six-hourly) and spatial (T255; interpolated to 0.75° regular horizontal) resolutions to analyse the large-scale conditions associated with the development of the storm.

The equivalent-potential temperature (θe) is the temperature a parcel of air would reach if all the water vapour in the parcel were to condense, releasing its latent heat, and the parcel was brought adiabatically to a standard reference pressure. Thus θe at the 850 hPa pressure level is used as an indicator of the combined effect of latent and sensible heat. It was computed using ERA Interim reanalysis data of temperature and relative humidity, following Bolton's formula (43) which uses the absolute temperature at the lifting condensation level given by his formula (22). For more details see Bolton (1980).

Maximum gust speeds and daily precipitation observed at meteorological stations located in Portugal were retrieved from preliminary reports published by Instituto Português do Mar e da Atmosfera, the Meteorological services from Portugal (IPMA, 2013). UK Met Office weather charts (available from www.wetter3.de/) and EUMETSAT satellite images (available from EUMETRAIN, www.eumetrain.org/) were used for the surface analysis of synoptic development, cloud patterns and mid-level moisture transport.

A European high-resolution gridded daily dataset of precipitation (E-OBS dataset; http://www.ecad.eu) developed as part of the European Union Framework 6 ENSEMBLES project with the aim of being used for climate change studies (Haylock et al., 2008) is also used on this study to evaluate daily extreme precipitation values observed at stations located in the Iberian Peninsula and their departures from the climatology. The daily precipitation sum dataset is made available on a 0.25° regular latitude–longitude grid covering the land-only area between 25 °N–75 °N and 40°W–75°E for the period 1950–2013. Daily precipitation sum for 1960-01-01 corresponds to the sum of the 1200 and 1800 values of 1960-01-01 to the 0000 and 0600 values of 1960-01-02. To evaluate the intensity for events occurring in Iberia in the month of January with a 20-year return period, the highest 1-day precipitation amount return values based on the period 1981–2000 for meteorological stations in the Iberian Peninsula were retrieved from ECA&D project dataset (Klein Tank et al., 2002; data available at http://www.ecad.eu).

Vertical profiles available were also used through the analysis of soundings of temperature, dew point temperature and wind and were obtained from the Department of Atmospheric Science of the University of Wyoming (http://www.uwyo.edu).

Finally an automatic cyclone detecting and tracking method is also used to objectively determine the genesis, development, and life cycle characteristics of low-pressure systems over the Northern Hemisphere extratropics. This is based on the cyclone detecting and tracking algorithm first developed by Trigo et al. (1999) for the Mediterranean region and later extended to a larger Euro-Atlantic region (Trigo, 2006). The scheme consists of the detection of minima in geopotential height fields that may be considered as possible storm centres and their tracking by looking for the nearest neighbour in the previous field, within an area defined by imposing thresholds to the maximum cyclone speed of 300 km/6 h in the westward direction and of 660 km/6 h in any other. If no cyclone centre is found within that area, then cyclogenesis is assumed to have occurred. Further details on the cyclone detecting and tracking algorithm can be found on Trigo (2006). It is here applied to 6-hourly geopotential data at 1000-hPa from ERA Interim reanalysis datasets described above.

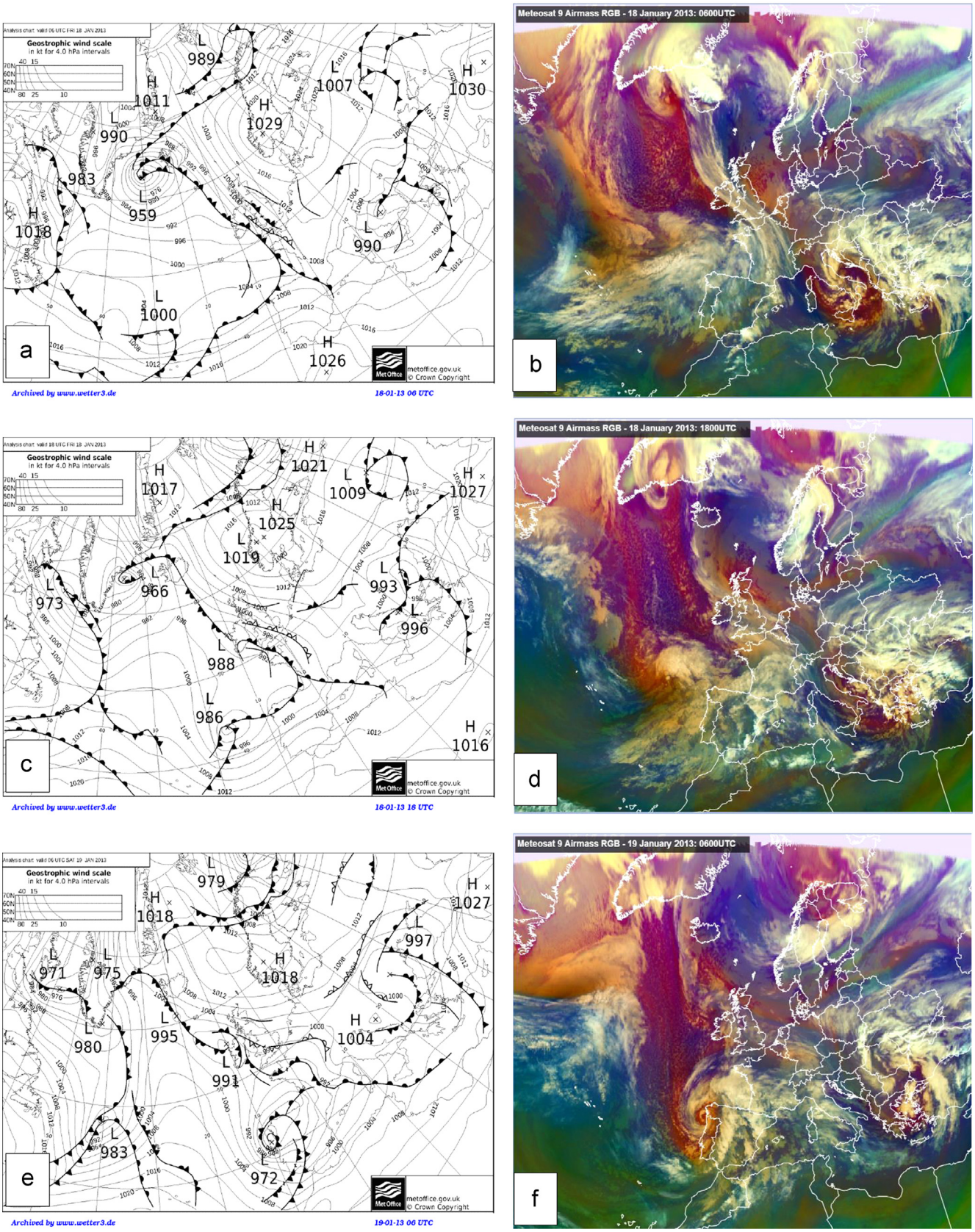

Fig. 1. (a) Surface analysis charts for 06 UTC on 18 January (courtesy of www.wetter3.de/). (b) Meteosat 9 composite image (often referred to as "air mass RGB") of the deepening low near peak strength and associated clouds near Iberia for 06 UTC on 18 January (courtesy of www.eumetrain.org/). (c) The same as (a) for 18 UTC on 18 January. (d) The same as (b) for 18 UTC on 18 January. (e) The same as (a) for 06 UTC on 19 January. (f) The same as (b) for 06 UTC on 19 January.

3. Cyclone trajectory and lifecycle characteristics

Windstorm Gong was located north of the Azores (43.5°N; 30°W) at 0600 UTC of 18 November (Fig. 1(a) and (b)) when it underwent a period of very rapid strengthening known as explosive development: the system's central pressure dropped from approximately 1001 hPa to a measured minimum pressure of 968 hPa 24 h later (Fig. 1). Following the criterion used by Sanders and Gyakum (1980), a storm exhibiting this type of explosive cyclogenesis is classified as explosive cyclone or 'bomb' (a rapidly deepening extratropical surface cyclone with a central pressure fall at sea level of at least (24 $\sin\varphi/\sin 60^\circ$) mbar in 24 h) and is always associated with strong winds.

Using the objective cyclone detecting and tracking scheme the low-pressure system's track and lifecycle characteristics were assessed. The low was first identified at 69°W and 40.5°N, at 18 UTC on 16 January 2013. The low pressure system propagated eastwards on the following days, embedded in the persistent westerly flow and experienced an explosive development on 18 January, just before reaching the northwestern tip of Iberia.

Fig. 2(a) shows the track of Gong (in black) together with the tracks of recent extreme storms Klaus (January 2009, in blue) and Xynthia (February 2010, in red) putting in evidence the similarities of their trajectories and/or characteristics. In fact, all three storm tracks are located at lower than usual latitudes (Pinto et al., 2009; Liberato et al., 2011, 2013; Ludwig et al., 2013). In addition all three storm tracks passed close to the Iberian Peninsula where they have their minimum pressure (marked with an open circle on Fig. 2(a)).

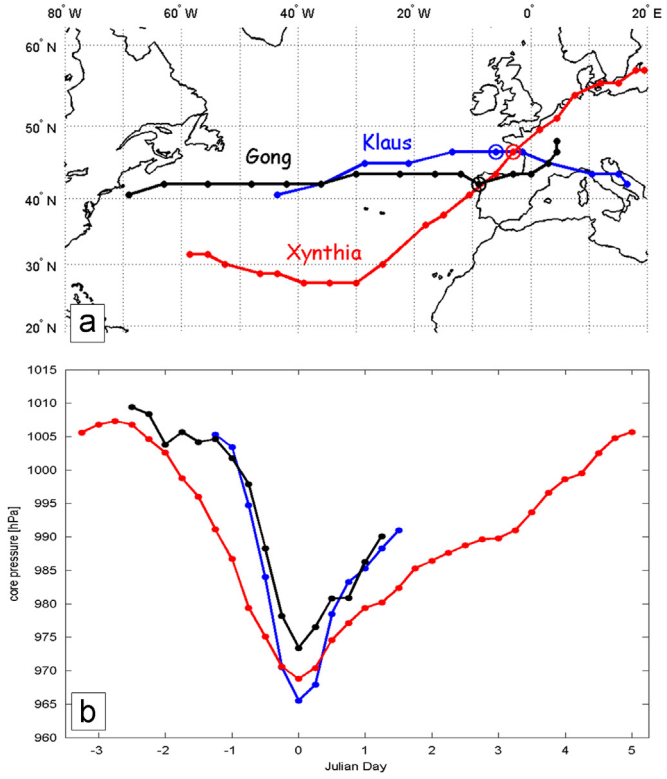

Fig. 2. (a) Cyclone tracks of recent extreme storms over the North Atlantic based on ECMWF ERA-Interim reanalysis data with dots indicating storms' location at six hour intervals: Gong (January 2013, in black), Klaus (January 2009, in blue) and Xynthia (February 2010, in red). The open circle marks the location of the minimum core pressure for each storm. (b) Core pressure evolution over the lifetime of each cyclone (core pressure in hPa). Dates are relative to the minimum core pressure time (zero Julian day).

Fig. 2(b) shows the evolution of the core pressure of the three storms evaluated in ERA-Interim reanalysis data; even though central pressure drops faster for storm Klaus (blue line) and to lower minima values for both storms Klaus (blue line) and Xynthia (red line), this high impact episode has also the characteristics of an extreme, rapidly deepening extratropical cyclone, usually known as "bomb". In this case, during the maturing stage, the rates of deepening exceeded 28 hPa per 24 h (from 1001.8 to 973.4 hPa during 18–19 January), which after being geostrophically adjusted to the reference latitude of 60°N (Trigo, 2006) is equivalent to 36 hPa per 24 h, confirming an exceptional event with 'bomb characteristics'.

The cyclone trajectory and central pressure values retrieved through the reanalysis have been confirmed by observations through surface analysis charts and satellite observations. Accordingly, Fig. 1 displays, for three time steps during the phase of rapid intensification of the storm, the surface analysis charts as derived by the UK Met Office (Fig. 1(a), (c) and (e)) and the Meteosat 9 composite images, often referred to as "air mass RGB", for the same time step (Fig. 1(b), (d) and (f)) (http://www.eumetrain.org/). These composite images make use of water vapour (6.2 μm and 7.3 μm), ozone (9.7 μm) and one thermal infrared (10.8 μm) channels, enhancing differences in temperature, moisture and cloud height: high/mid-level appear white/pinkish, while dry stratospheric air is revealed in reddish colours. Bluish colours show the water vapour content in a layer between approximately 200 and 500 hPa. Fig. 1(b), (d) and (f) show clearly the cloud structures associated with the cyclone during its development to the moment of making landfall at the Portuguese coast. A band of clouds approaching Iberia and running parallel to the cold front may be assigned to the warm conveyor belt of the cyclone system. The cold conveyor belt is also identified through a region without clouds and appearing in reddish colour indicating dry air/low tropopause in this type of composite image (Fig. 1(f)). This may be explained through descending dry air, associated with the dry intrusion, which is a common feature during the development phase of extratropical cyclones (Browning, 1997).

During the following 30 h the low pressure system tracked to central France, where it dissipated.

4. Large-scale synoptic evolution and dynamics

4.1. Surface cyclone, baroclinicity and upper-level jet stream

At 18 UTC on 16 January 2013, Gong appeared as a developing cyclone, with an analysed core pressure below 1010 hPa, at 69°W and 40.5°N, just off the North American coast (Fig. 2(a)). During the following 24 h the cyclone moved zonally eastwards, on a region of enhanced low level meridional temperature and humidity gradient, while simultaneously the upper-level flow over the western North Atlantic was anomalously strong (with a jet maximum speed of over 90 m s^{-1}), remained almost stationary and also zonally oriented. These are shown in the thermohydrodynamical reanalysis fields on Fig. 3(a) and (b), which represent, for 18 UTC on 17 January 2013, the maps of the θe, at 850 hPa, the MSLP and the cyclone trajectory (Fig. 3(a)) and the upper air jet stream described through the wind speed and divergence at the 250 hPa level (Fig. 3(b)). The surface cyclone core position at each time step is indicated in each panel by a black square. The following panels show that in the case of Gong's development, similarly to Klaus' explosive development (Liberato et al., 2011), the low-pressure system path followed very closely a region of low level baroclinicity characterized by the largest θe gradient, within the transition between subtropical and polar air masses (Fig. 3(c), (e) and (g)). By 18 January (06 UTC and 18 UTC), the cyclone is

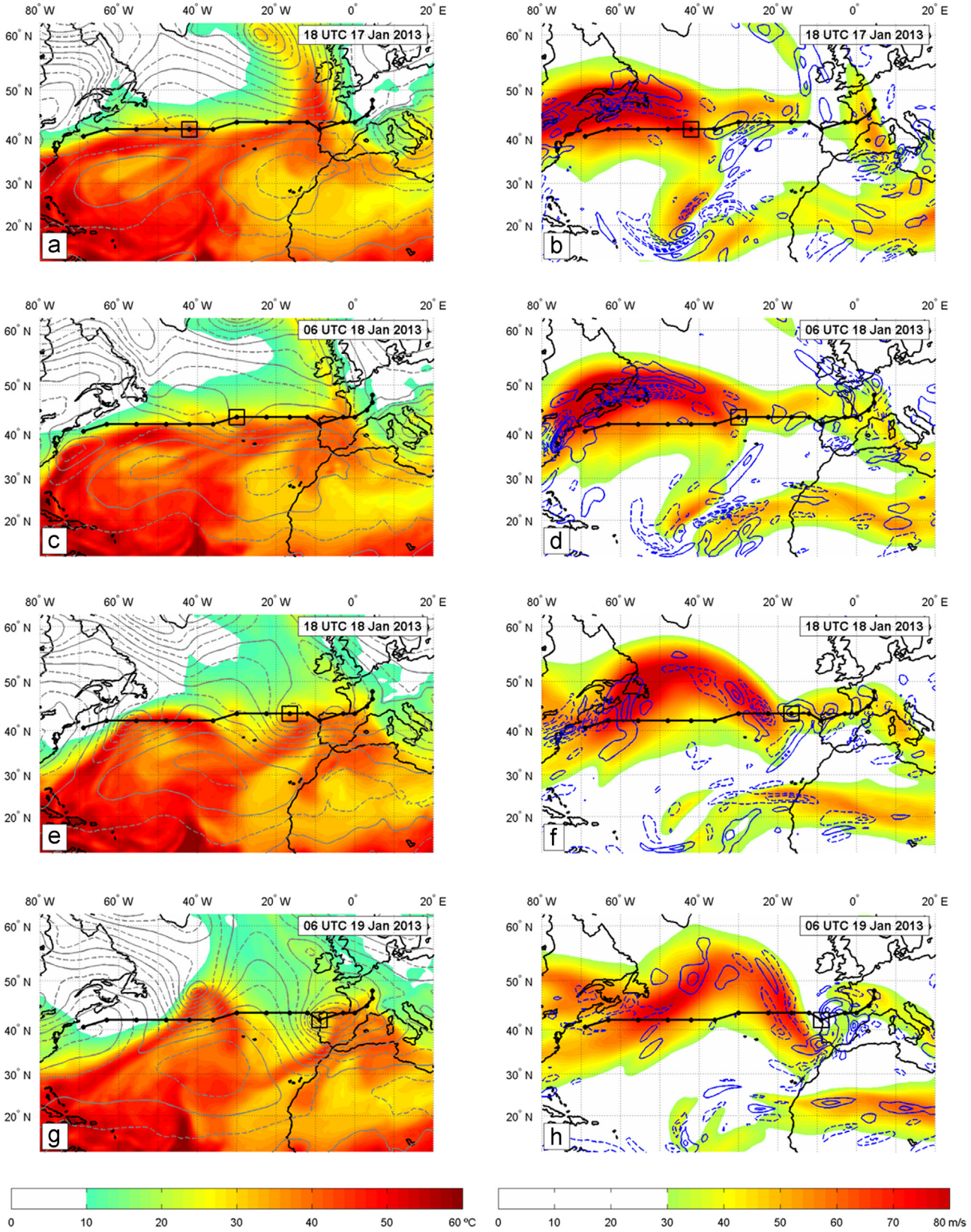

Fig. 3. Large-scale conditions associated with the development of the cyclone Gong. (a) Equivalent potential temperature (θe) field at 850 hPa (shaded; °C, see colorbar) and the mean sea level pressure (MSLP) field (contour interval 4 hPa) for 18 UTC on 17 January 2013. (b) Wind speed (shaded; m s^{-1}, see colorbar) and divergence (contours every 2×10^{-5} s^{-1}, delimiting areas above 2 (solid lines) and below −2 (dashed lines)) at the 250 hPa level for 18 UTC on 17 January 2013. (c) The same as (a) for 06 UTC on 18 January. (d) The same as (b) for 06 UTC on 18 January. (e) The same as (a) for 18 UTC on 18 January. (f) The same as (b) for 18 UTC on 18 January. (g) The same as (a) for 06 UTC on 19 January. (h) The same as (b) for 06 UTC on 19 January. Cyclone track is displayed in black and position at corresponding time is marked with a square.

located at the tip of a broad area with high values of θe (Fig. 3(c) and (e)), called a θe ridge. These figures reveal high values of θe at 850 hPa in the warm sector of the surface disturbance. Since the θe of an air parcel increases with increasing temperature and increasing moisture content, these results confirm the occurrence of a maximum of latent and sensible heat availability in the lower troposphere which support the contribution of moist diabatic processes, such as latent heat release by cloud condensation processes, in the intensification of the windstorm (Chang et al., 1984; Pinto et al., 2009; Fink et al., 2012, Liberato et al., 2011, 2013; Ludwig et al., 2013).

It is well known that another important factor in the explosive development of an extratropical storm is the relative position of the storm and the upper-level jet which may steer the storm (e.g., Uccellini and Johnson, 1979; Baehr et al., 1999). From 18 UTC on 17 January to 18 UTC on 18 January 2013 (Fig. 3(b), (d) and (f)) the cyclone crossed from the warm to the cold side of the jet, to its poleward side over the central North Atlantic, north of the Azores, and its rapid development began as it moved from the maximum velocity region to the left jet streak exit region (Fig. 3(f)), towards a region of enhanced upper-air divergence values ($>2\times10^{-5}\ s^{-1}$) (Fig. 3(f) and (h)). It is evident, at 18 UTC on 18 January, the coma-shaped, high values of upper-air divergence in the vicinity of the cyclone position (Fig. 3(f)) while at the surface the tongue of warm and moist air still supplies from lower levels the cyclone with energy needed for the explosive growth of this damaging windstorm (Fig. 3(e)).

It is worth remarking that both Gong and Klaus experienced the explosive development approximately on the same region, north of the Azores (Fig. 2(a)). Such 'bombs', like Gong and Klaus, are not unusual over the North Atlantic Basin (Sanders, 1986; Trigo, 2006), however they are very rare at these low latitudes (e.g., Pinto et al., 2009; Liberato et al., 2011).

Fig. 4 shows the evolution of radiosonde profiles at 00 UTC 19 January for Corunna, Spain, which confirm the above mentioned lower troposphere warm, moist air. The skew-T log-P diagram shows clearly the existence of a deep layer of warm, saturated moist air mass extending from the surface to around 600 hPa. Additionally the air appears to be stable in the lowest 50 hPa of the atmosphere, which may have led to orographic enhancement of rainfall over northwestern Iberia. A cold, stable dry air mass associated with a dry intrusion (see also description of Fig. 1(d) and (f)) may be found on the overlaying layer around 600–550 hPa.

This cold, dry stratospheric intrusion may also be diagnosed through the potential vorticity (PV) field, since it is characterized by high values of PV. It should be noted that stratospheric air masses are usually characterized by PV values higher than 2 PVU (2 potential vorticity units ($PVU=1\times10^{-6}\ K\ kg^{-1}\ m^2\ s^{-1}$)). Fig. 5 shows a three-dimensional analysis of the PV field for the moment of maximum intensification and higher impact on Iberia (06 UTC 19 January 2013). The upper-level PV field (at 250 hPa) together with the geopotential height of the 500 hPa surface is shown in Fig. 5(a), revealing a pronounced cyclonic PV streamer which approached Iberia, from northwest, with high values (greater than 7 PVU at 250 hPa) and reaching unusual low latitudes (35°N) (Wernli and Sprenger, 2007; Martius et al., 2007). At the time of the maximum intensification it is located within the axis of the 500 hPa long-wave trough (Fig. 5(a)) with PV values over 2 PVU at 600 hPa and vertically aligned with the surface cyclone, which is characterized by PV values over 2 PVU and relative humidity values over 80% at 42°N (Fig. 5(b)) and at 9°W (Fig. 5(c)). The vertical meridional (Fig. 5(b)) and zonal (Fig. 5(c)) cross sections make evidence of the simultaneous presence of a low-level and an upper-level PV anomaly, confirming that the surface low pressure system and the upper level PV anomaly do interact. This result is

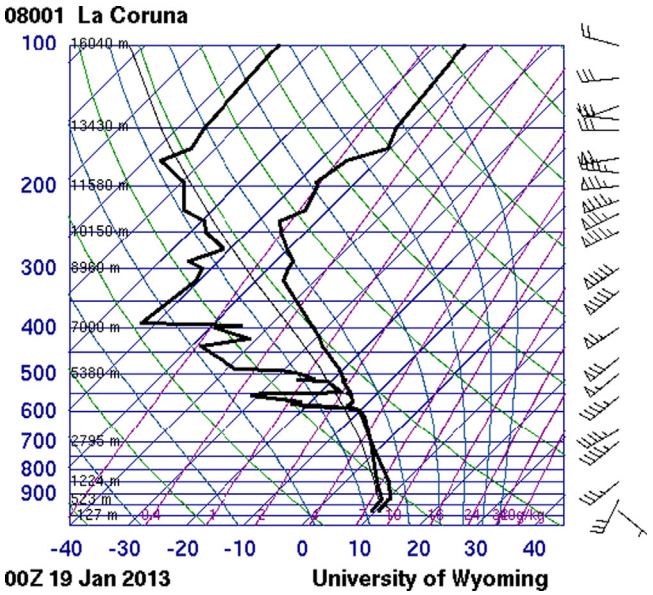

Fig. 4. Skew-T log-P diagram as derived from the sounding of wind, temperature and dew point temperature on the 19 January 2013 (00 UTC) at the station of Corunna (Spain) - northwestern tip of Iberia (http://www.uwyo.edu).

in agreement with previous studies which showed that the interactions between upper-level PV anomalies and diabatically induced low-level PV anomalies can lead to an intensification of the cyclogenesis process (Hoskins et al., 1985) and to the occurrence of a so called PV tower, which is a typical characteristic of strong extratropical cyclones (e.g., Wernli et al., 2002; Campa and Wernli, 2012).

4.2. The influence of the AR on Gong's intensification

This severe weather, high impact event was characterized not only by strong wind gust but also by continuous, heavy precipitation and flooding in Portugal (IPMA, 2013). This also motivated also the investigation on the origin of the moisture responsible for the anomalous continuous rainfall on 18–19 January 2013 over Portugal.

When extreme hydrometeorological extremes are considered, several recent works have devoted a particular attention to the important role played by atmospheric rivers (ARs) (e.g. Ralph and Dettinger, 2011). ARs are narrow, elongated bands of water vapour (Newell et al., 1992; Ralph et al., 2006), which cross the mid-latitudes in each hemisphere and where approximately 90% of poleward atmospheric water vapour transport is concentrated (Zhu and Newell, 1998). ARs are characterized as regions with: (i) concentrations of integrated water vapour in the atmospheric column of more than 2 cm (Ralph et al., 2004); and (ii) wind speeds greater than 12.5 m s^{-1} in the lowest 2 km of the atmosphere (Ralph and Dettinger, 2011). The connection between ARs and heavy precipitation events and floods has been shown for California, in the North American west coast (Ralph et al., 2004, 2006), but also for events in Europe, for example in Norway (Stohl et al., 2008), in the United Kingdom (Lavers et al., 2011) and in Portugal (Liberato et al., 2012). In all these cases it was shown that the large amounts of water vapour transported by the ARs led to extreme precipitation events and flooding since these structures can trigger elongated convective storms over the oceans and heavy orographically forced rain events when making landfall.

In this section the analysis makes evidence of the presence of an AR coincidently with the development and intensification of the low pressure system. Fig. 6 shows, for the period from 18 UTC

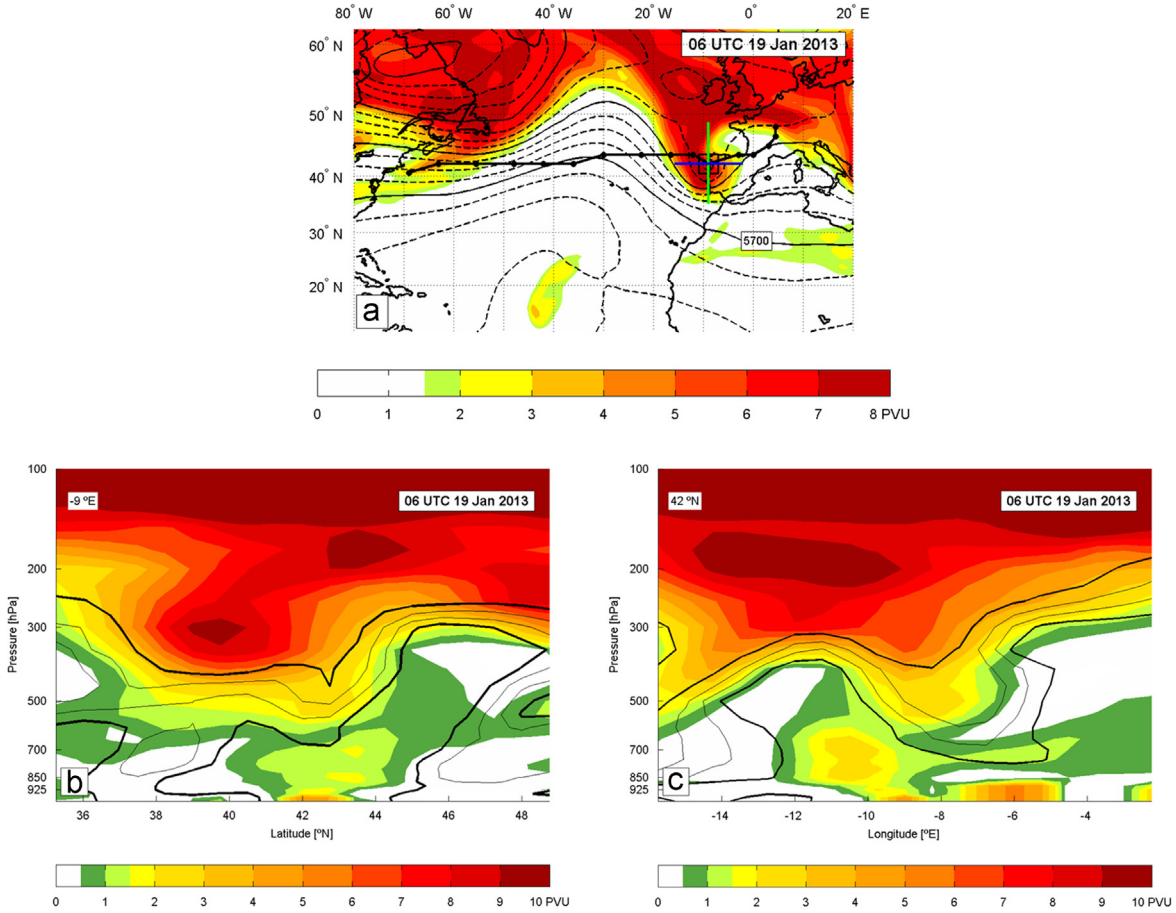

Fig. 5. (a) Upper tropospheric potential vorticity distribution (shaded; PVU) at 250 hPa and geopotential height at 500 hPa (contours every 80 gpm) for 06 UTC on 19 January 2013. Cyclone track is displayed in black and position at corresponding time is marked with a square. Green and blue lines are the location along which the cross sections were taken. (b) South–north oriented cross section at longitude 9°W (green line on a) of PV distribution (shaded; PVU) and relative humidity field (contours every 20% from 20 to 80%; 20% and 80% contours are thicker). (c) The same as (b) for west-east oriented cross section at latitude 42°N (blue line on a). Notice the different colorbar in (a).

17 January to 06 UTC 19 January 2013, the TCWV and divergence at 900 hPa (left panels) and the MSLP and wind at 900 hPa (right panels), making clear evidence of the occurrence of a persistent long plume of moist air with values of TCWV over 20 mm during the whole period in consideration, together with a persistent eastward low level flow of relatively strong winds (wind speed greater than 12.5 m s^{-1}; right panels of Fig. 6) crossing the North Atlantic basin towards Iberia.

The influence of advection of tropical moisture air masses on rapid extratropical cyclogenesis has recently been highlighted on other extreme windstorms such as Klaus (Knippertz and Wernli, 2010; Liberato et al., 2011) and Xynthia (Liberato et al., 2013). Additionally, Knippertz and Wernli (2010) suggested storm Klaus would be a possible example of 'tropical moisture export' (TME), showing that the development of Klaus was embedded in a massive TME event which originated over the entire central and western tropical Atlantic and then converged into the genesis region of the cyclone. All these examples suggest the connection between rapid extratropical cyclogenesis and ARs, which will deserve further climatological research.

Fig. 6 (left panels) also shows low-level moisture convergence over Iberia, with values below -2×10^{-5} s^{-1}, at 900 hPa, which are favourable large-scale conditions for vertical movements (uplift mechanism, which induces deep convection activity), supporting the idea that the large-scale conditions over Portugal were optimal for anomalous continuous and eventually strong rainfall on 18–19 January 2013. These facts support the hypothesis that large-scale forcing was crucial to the enhancement of this extreme rainfall and flood event on Iberia.

Liberato et al. (2012) studied the connection between an AR and a heavy precipitation event in Portugal, showing by means of a Lagrangian diagnosis method developed by Stohl and James (2004, 2005) how long-range transport of water vapour from the subtropics was important in setting up the large-scale conditions required for a particular extreme precipitation event in Portugal. Results shown in this section also corroborate the important role of the AR on the moisture content and availability on this extreme event in accordance with Liberato et al. (2012).

5. Meteorological and socioeconomic impacts

Through the afternoon and evening of 18 January 2013 the Portuguese meteorological services issued a series of meteorological warnings, from yellow, to orange and later to red at the dawn and morning of Saturday, 19 January 2013, due to extreme precipitation and wind forecast.

Fig. 7 describes the meteorological impacts of storm Gong according to the values measured at the Portuguese meteorological stations and informed on the IPMA (2013) report. The wind impacts of storm Gong affected mainly the centre and south of Portugal mainland as shown on Fig. 7(b). The rapid drop in pressure described previously caused wind speeds to rise, reaching the maximum of "Force 12" on the Beaufort scale in some

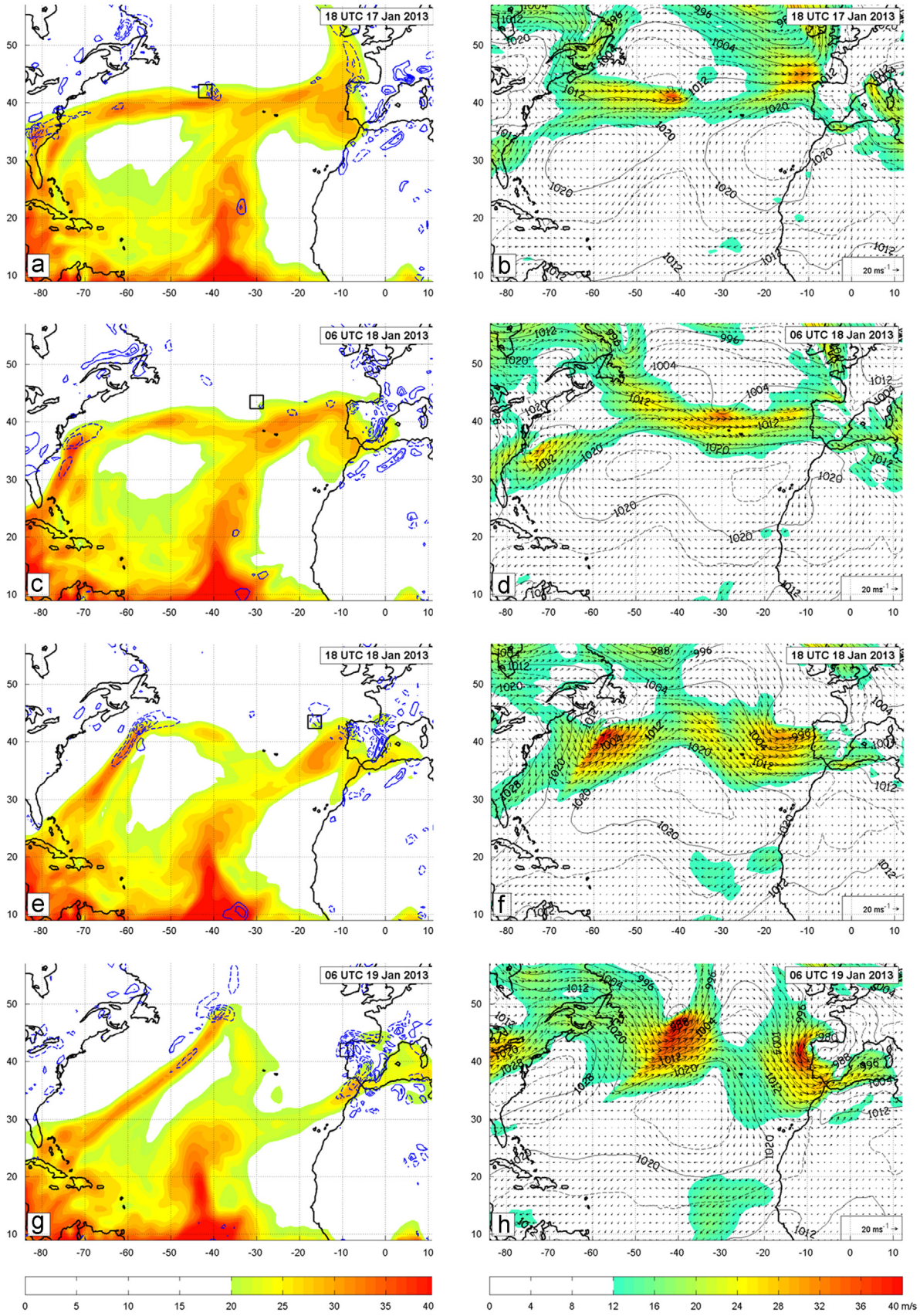

Fig. 6. (a) Total column water vapour (TCWV) (shaded; mm, see colorbar) and divergence (contours every 2×10^{-5} s^{-1}, delimiting areas above 2 (solid lines) and below -2 (dashed lines)) at the 900 hPa level for 18 UTC on 17 January 2013. (b) MSLP field (contour interval 4 hPa) and the vector wind and wind speed at 900 hPa (shaded; m s^{-1}, see colorbar) for 18 UTC on 17 January 2013. (c) The same as (a) for 06 UTC on 18 January. (d) The same as (b) for 06 UTC on 18 January. (e) The same as (a) for 18 UTC on 18 January. (f) The same as (b) for 18 UTC on 18 January. (g) The same as (a) for 06 UTC on 19 January. (h) The same as (b) for 06 UTC on 19 January.

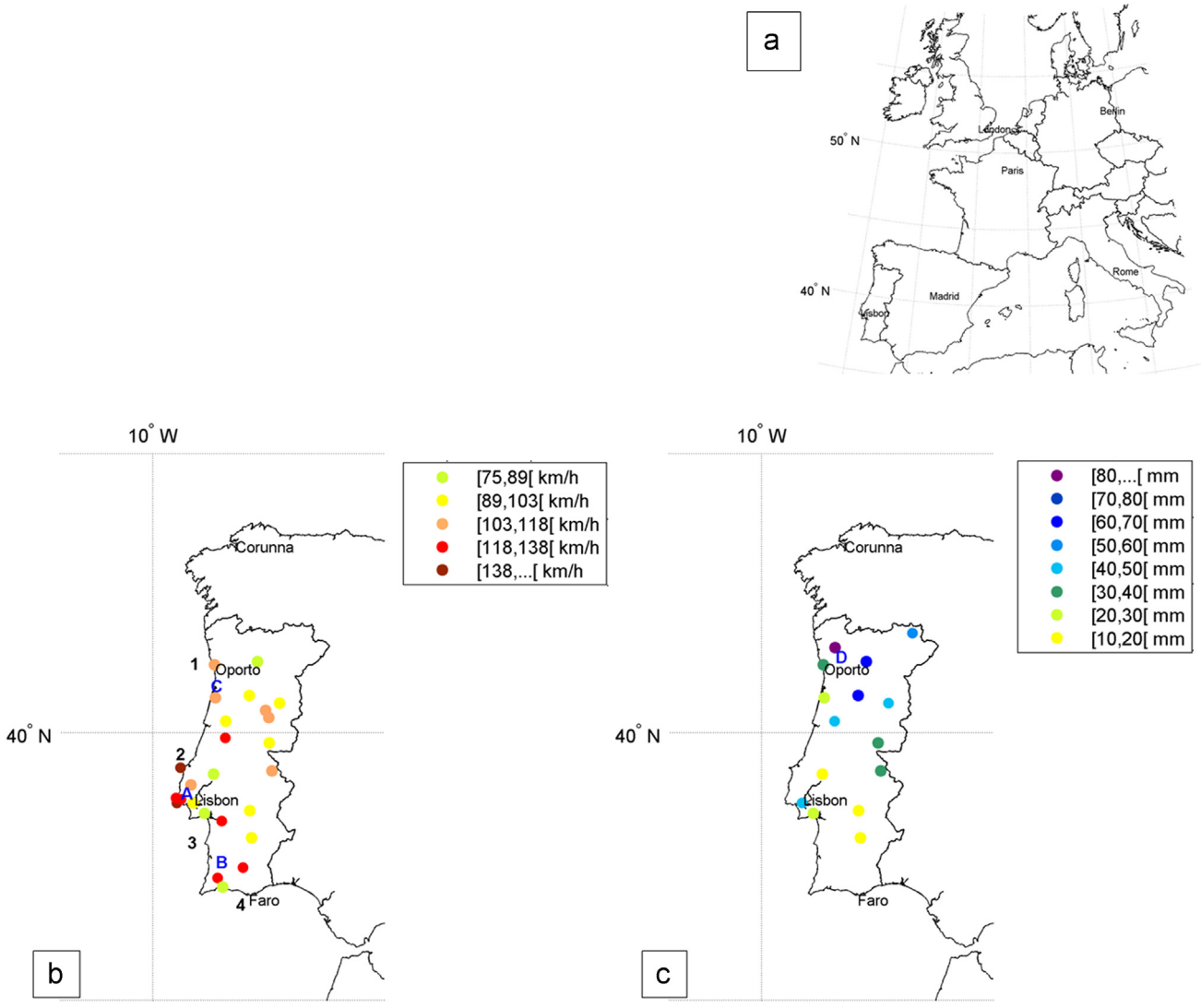

Fig. 7. (a) Small map of Europe. (b) Maximum wind gusts (in km h^{-1}) at meteorological stations in Portugal, for 19 January 2013. Only stations where recorded values surpassed Beauford wind force 9 are marked. Colour scale represents the Beaufort wind force scale from 9 (strong gale; $\geq$ 75 km h^{-1}) to 12 (hurricane force; $\geq$ 118 km h^{-1}). The letters A, B and C identify locations of Fig. 10(a)–(c), respectively. The numbers 1–4 identify the buoy locations of Table 1. (c) Precipitation totals (in mm) measured between 09 UTC of 18 January and 09 UTC of 19 January at the Portuguese meteorological stations (IPMA, 2013).

locations. At this stage wind gusts of over 90 km h^{-1} were registered all over the territory of Portugal mainland and severe storm force gusts of over 118 km h^{-1} ("Beaufort wind force 12") were measured at low-level stations on the western coast of Portugal (Fig. 7(b)), accompanied by heavy rain and consequent flooding, whilst snow fell strongly across the Serra da Estrela Mountains (IPMA, 2013). Fig. 7(c) reflects the 24 h rainfall measured at the Portuguese meteorological stations (IPMA, 2013) for 19 January 2014, that is, precipitation values measured between 09 UTC 18 January and 09 UTC 19 January. It should be noted that daily precipitation records obtained in Portugal for any given day *n* correspond to the precipitation registered between 09 UTC of day *n-1* and 09 UTC of day *n*. This figure (Fig. 7(c)) shows that on the north and centre of Portugal there have been daily totals of more than 30 mm, which on several locations exceeded the 60 mm, with a maximum of 89.0 mm in Braga (41.55°N; −8.42°E). To put these values in perspective and show the significance of this heavy precipitation event for the hydrology of the region it is important to compare with the climatology of the Iberian Peninsula. The European high-resolution gridded daily dataset of precipitation (Haylock et al., 2008) has been used here to compute the monthly climatological (for the 1981–2010 period) accumulated precipitation values for Iberia, for January (Fig. 8(a)) and the corresponding values for 18 January 2013 (Fig. 8(b)). As previously stated, the 18 January daily precipitation sum on this dataset corresponds to the sum of the 1200 and 1800 values of 2013-01-18 to the 0000 and 0600 values of 2013-01-19, thus being comparable to the values on Fig. 7(c). The analysis of Fig. 8 confirms that around 20–25% of the local monthly climatological rainfall occurred during 24 h on the northwest of Iberia. Furthermore, in order to better evaluate the intensity and frequency of more rare events, return values can be calculated. Values plotted on the map of Fig. 9 represent the highest 1-day precipitation amount 20 year return values, for the month of January, based on the period 1981–2000, for meteorological stations in the Iberian Peninsula as retrieved from ECA&D project dataset (Klein Tank et al., 2002; data available at http://www.ecad.eu). Shown here are only those stations that passed the homogeneity test and for which the Gumbel distribution provides

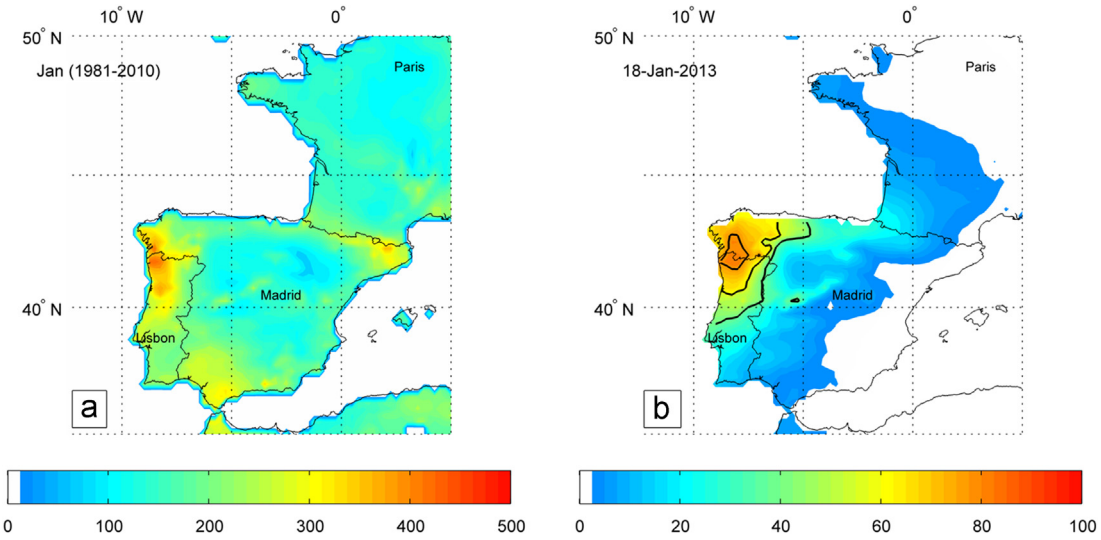

Fig. 8. (a) High-resolution gridded climatological (for the 1981–2010 period) accumulated precipitation values (in mm) for Iberia, for January. (b) Precipitation sum of the 1200 and 1800 values of 2013-01-18 to the 0000 and 0600 values of 2013-01-19. Thick contours show 40, 60 and 80 mm. (E-OBS dataset available at http://www.ecad.eu).

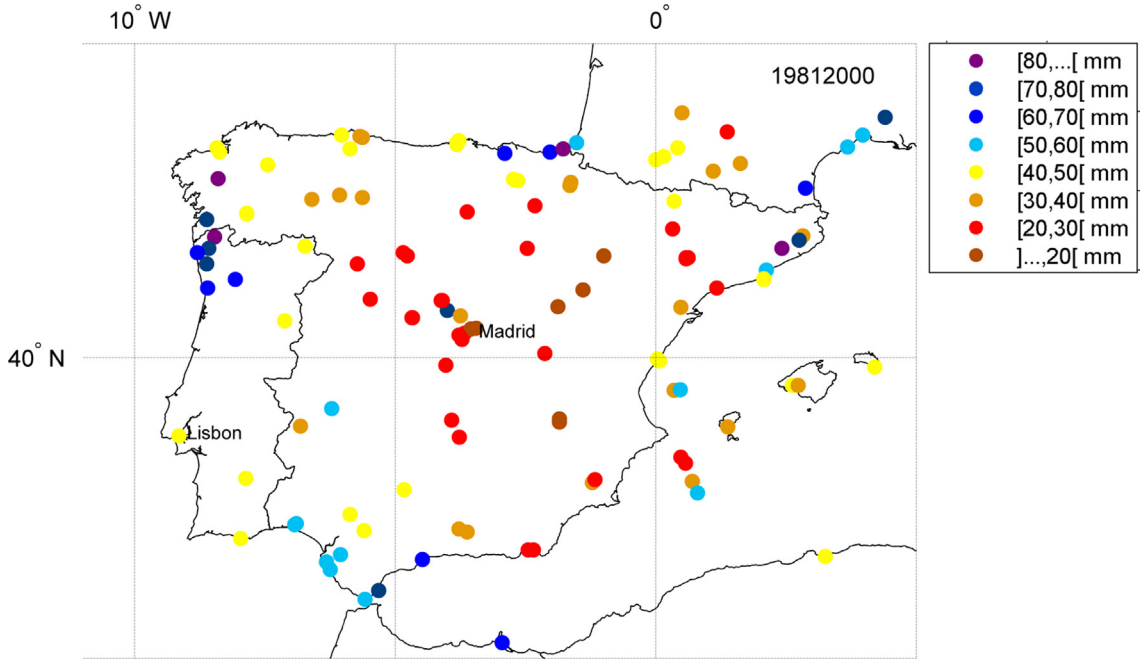

Fig. 9. Highest 1-day precipitation amount for meteorological stations in the Iberian Peninsula. Return values evaluate the intensity for events that occur in the month of January once in 20 years based on the period 1981–2000 (Data available at http://www.ecad.eu).

an acceptable fit. More details and a description of the goodness-of-fit test that has been applied are given in the project information (Klein Tank et al., 2002; http://www.ecad.eu). This figure makes additional evidence of the exceptionality of this heavy precipitation event on the northwestern Iberia.

Correspondingly, windstorm Gong caused considerable socio-economic damage and huge insured losses in Portugal mainland where winds were sufficiently strong to disrupt transportations, to blow off roofs and essentially to cause some structural damage due to uprooted trees. The storm was responsible for the downfall of thousands of trees on some of the Portuguese national forests, some of them centenary trees in Sintra natural parks (Expresso, 2013a; Fig. 10(a)), on the University of Coimbra Botanic Garden (Expresso, 2013b) and on the Buçaco National Forest (Público, 2013a). Two fatalities were reported in addition to huge adverse impacts on buildings, cars and on the national electricity network, which has seen more than 11,000 km of wires being damaged. Many locations lost access to electricity as a direct consequence of the event with nearly 1 million of homes affected, corresponding to circa 2.6 million people without access to electricity and communications, some of them for several days (Correio da Manhã, 2013a, b). The severe winds were also responsible for the destruction of hundreds of greenhouses (Fig. 10(b)) and of the agricultural year production on more than a thousand farms, affecting an area of more than 900 ha (Público, 2013b; AGROPORTAL, 2013). The overall number of claims was estimated at more than 40,000 with insured losses amounting to over EUR 100 million according to the Portuguese Association of Insurance (Associação Portuguesa de Seguradores (APS, 2013a, b)).

The adverse effect of the strong winds was also noticeable on the Atlantic Ocean with high seas and large waves near the Portuguese coast. During the morning of 19 January the

Fig. 10. Photos documenting the impact of storm Gong, 19 January 2013, showing: (a) Example of damage in Sintra, Portugal(courtesy of Emília Reis). (b) Greenhouses disruption at Odemira, Portugal (photograph of Tiago Canhoto/courtesy of Lusa). (c)The merchant ship "MERLE" stranding on the Torreira beach, Portugal (photograph of Paulo Novais/courtesy of Lusa). (d)–(e) The floods of Ave river at Amieiro Galego (courtesy of Carlos Valente). (f) Identification of previous floods levels at Amieiro Galego (courtesy of Américo Fernandes). The sites are identified with letters from "A" to "D" on the maps of Fig. 7.

Table 1
Values of significant and maximum wave height (m) recorded on the Portuguese Hydrographic Institute buoys network. The numbers marked on the map of Fig. 7(b) indicate the approximate location of the 4 buoys.

Buoy	Significant wave height (m)	Maximum wave height (m)
Leixões (1)	9.7	15.6
Nazaré (2)	12.0	19.4
Sines (3)	9.8	17.5
Faro (4)	4.5	9.1

Coordinating Centre for Maritime Search and Rescue in Lisbon (Lisboa-MRCC) and the Aveiro Port Authority led a rescue operation of the crew of the merchant ship "MERLE" with 84 m length, and flag of Cook islands, which was unruly and ended up stranding on the Torreira beach, near Aveiro (Portal da Marinha, 2013a; Fig. 10(c)). It would take more than 2 months to finally remove the vessel from the beach (Público, 2013c). According to the Hydrographic Institute, on the 19 January the 4 buoys from the network registered high values of significant wave height, from the W–NW, with a maximum recorded value of 19.4 m in the oceanic buoy off the coast of Nazaré (Table 1). It is worth noting that the maximum of 17.5 m of the wave's height in Sines corresponds to the highest value ever recorded by the Sines buoy in the last 25 years (Portal da Marinha, 2013b).

The continuous, heavy precipitation during the afternoon of 18 January were responsible for flooding on several locations of the north of Portugal, motivating the closure of several roads and bridges (Correio da Manhã, 2013c; Fig. 10(d) and (e)). Fig. 10(f) shows a zoom of the house window on Fig. 10(e), where the height of previous floods has been registered, showing that the level of this January 2013 flood event on this location (letter D on the map of Fig. 7(c)) has almost equalled the height of previous floods on 1 April 1962 and on 22 December 1909, the latter being the so-called "century floods".

6. Summary and concluding remarks

Extratropical cyclones are one of the most prominent features of the midlatitude climate and represent a major mechanism for poleward transport of heat and moisture (Peixoto and Oort, 1992). The occurrence of extreme windstorms is considered as one of the major natural catastrophes in the extratropics, being one of the most costly natural hazards in Europe, responsible for substantial socioeconomic damages and fatalities. As countries in southwestern Europe are rarely affected by severe windstorms, a comprehensive assessment of the large-scale synoptic evolution and of the dynamical mechanisms that forced the unusual explosive development of windstorm Gong (18–19 January 2013) is presented in this paper, together with a description of the associated meteorological and socioeconomic adverse impacts. This severe weather, high impact event was characterized not only by wind gust of "Force 12" on the Beaufort wind scale but also by continuous, heavy precipitation and flooding in Portugal.

The low pressure system was formed on the western North Atlantic and underwent a typical mid-latitude explosive development, closely associated with the crossing of the polar jet stream. However this development occurred on the southern edge of the North Atlantic storm track, at lower latitudes than usually. In fact windstorm Gong underwent an explosive development with 'bomb' characteristics between the Azores and the Iberian Peninsula, with a deepening rate of 36 hPa in 24 hours, unusually high for these latitudes.

Results show that the main atmospheric driving factors for the explosive intensification of the cyclogenesis process of Gong storm are in agreement with classical studies on extratropical cyclones, that is: (i) the occurrence of upper-level horizontal divergence at the entrance and exit region of a jet streak (Uccellini and

Johnson, 1979); (ii) the crossing of the cyclone from the warm to the cold side of the jet stream (Baehr et al., 1999); (iii) enhanced baroclinicity and the contribution of moist diabatic processes, such as the availability of latent heat energy (Chang et al., 1984); (iv) interactions between upper-level PV anomalies and diabatically induced low-level PV anomalies (Hoskins et al., 1985). Furthermore in this study it is shown that the explosive development at such low latitudes is also driven by: (i) the southerly displacement of a strong polar jet stream; and (ii) the presence of an AR, that is by a (sub)tropical moisture export over the western and central (sub)tropical Atlantic which converges into the cyclogenesis region and then moves along with the storm towards Iberia, which is in agreement with recent findings (Knippertz and Wernli, 2010; Liberato et al., 2011).

Recent studies suggest that the total number of extratropical cyclones may decrease on this region, though the intensity of extreme cyclones may increase (Ulbrich et al., 2009 and references therein). This is particularly true for cyclones developing on the southern edge of the North Atlantic storm track, which may be then more strongly diabatically driven than under present climate conditions due to future warming SSTs, enhancement of moisture availability and potentially enhanced latent-heat release, thus increasing the windstorm risk for southwestern Europe (Liberato et al., 2013; Ludwig et al., 2013). The evidence and detailed analysis of extreme extratropical cyclones such as Klaus, Xynthia and Gong as well as the uncommon large-scale atmospheric circulation conditions prior to and during their explosive development and physical mechanisms that favoured their occurrence is then fully justified on the context of weather and climate extreme variability research.

Acknowledgments

This work was supported through project STORMEx FCOMP-01-0124-FEDER-019524 (PTDC/AAC-CLI/121339/2010) by FEDER (Fundo Europeu de Desenvolvimento Regional, Europe) funds through the COMPETE (Programa Operacional Factores de Competitividade) Programme and by national funds through FCT (Fundação para a Ciência e a Tecnologia, Portugal). The author thanks the European Centre for Medium-range Weather Forecasts for providing the ERA-Interim reanalysis data. The author also acknowledges the E-OBS precipitation dataset from the EU-FP6 project ENSEMBLES (http://ensembles-eu.metoffice.com) and the data providers in the ECA&D project (http://www.ecad.eu). The author is grateful to Joaquim G. Pinto, Alexandre M. Ramos and Isabel F. Trigo for their helpful discussions and comments. The author also acknowledges also the editor and two anonymous reviewers for their constructive comments that helped to improve the manuscript.

References

AGROPORTAL, March 19, 2013. Número de explorações agrícolas afectadas pelo temporal de Janeiro aumenta para 1.300. ⟨http://www.agroportal.pt/⟩, (last access: 29.12.13) (in Portuguese).

APS, March 8, 2013a. Ascende já a 83 milhões de euros o custo do temporal para as seguradoras. ⟨https://www.apseguradores.pt/⟩ (last access: 29.12.13) (in Portuguese).

APS, August 13, 2013b. Seguradoras reforçam resultados e rácio de solvência no 1° semestre do ano. ⟨https://www.apseguradores.pt/⟩ (last access: 29.12.13) (in Portuguese).

Baehr, C., Pouponneau, B., Ayrault, F., Joly, A., 1999. Dynamical characterization of the FASTEX cyclogenesis cases. Q. J. R. Meteorol. Soc. 125, 3469–3494. http://dx.doi.org/10.1002/qj.49712556117.

Bolton, D., 1980. The computation of equivalent potential temperature. Mon. Weather Rev. 108, 1046–1053.

Browning, K.A., 1997. The dry intrusion perspective of extra-tropical cyclone development. Met. Appl. 4, 317–324.

Campa, J., Wernli, H., 2012. A PV perspective on the vertical structure of mature midlatitude cyclones in the Northern Hemisphere. J. Atmos. Sci. 69, 725–740.

Chang, C.B., Pepkey, D.J., Kreitzberg, C.W., 1984. Latent heat induced energy transformations during cyclogenesis. Mon. Weather Rev. 112, 357–367.

Compo, G.P., Whitaker, J.S., Sardeshmukh, P.D., Matsui, N., Allan, R.J., Yin, X., Gleason, E., Vose, J.r., Rutledge, R.S., Bessemoulin, G., Brönnimann, P., Brunet, S., Crouthamel, M., Grant, R.I., Groisman, A.N., Jones, P.Y., Kruk, P.D., Kruger, M.C., Marshall, A.C., Maugeri, G.J., Mok, M., Nordlki, H.Y., Ross, T.F., Trigo, R.M., Wang, X.L., Woodruff, S.D., Worley, S.J., 2011. The Twentieth Century Reanalysis Project. Q. J. R. Meteorol. Soc. 137 (654), 1–28. http://dx.doi.org/10.1002/qj.776.

Correio da Manhã, January 21, 2013a. Vento faz estragos de milhões. ⟨http://www.cmjornal.xl.pt/⟩ (last access: 29.12.13) (in Portuguese).

Correio da Manhã, February 19, 2013b. Prejuízos de 105 milhões de euros no temporal. ⟨http://www.cmjornal.xl.pt/⟩ (last access: 29.12.13) (in Portuguese).

Correio da Manhã, January 19, 2013c. Temporal gera caos no Porto e em Braga. ⟨http://www.cmjornal.xl.pt/⟩ (last access: 29.12.13) (in Portuguese).

Dee, D.P., Uppala, S.M., Simmons, A.J., Berrisford, P., Poli, P., Kobayashi, S., Andrae, U., Balmaseda, M.A., Balsamo, G., Bauer, P., Bechtold, P., Beljaars, A.C.M., van de Berg, L., Bidlot, J., Bormann, N., Delsol, C., Dragani, R., Fuentes, M., Geer, A.J., Haimberger, L., Healy, S.B., Hersbach, H., H'olm, E.V., Isaksen, L., Kallberg, P., Köhler, M., Matricardi, M., McNally, A.P., Monge-Sanz, B.M., Morcrette, J.-J., Park, B.-K., Peubey, C., de Rosnay, P., Tavolato, C., Thépaut, J.-N., Vitart, F., 2011. The ERA-Interim reanalysis: configuration and performance of the data assimilation system. Q. J. R. Meteorol. Soc. 137, 553–597. http://dx.doi.org/10.1002/qj.828.

Domínguez-Castro, F., Trigo, R.M., Vaquero, J.M., 2013. The first meteorological measurements in the Iberian Peninsula: evaluating the storm of November 1724. Clim. Change 118, 443–455. http://dx.doi.org/10.1007/s10584-012-0628-9.

Donat, M.G., Renggli, D., Wild, S., Alexander, L.V., Leckebusch, G.C., Ulbrich, U., 2011. Reanalysis suggests long-term upward trends in European storminess since 1871. Geophys. Res. Lett. 38.

Expresso, January 20, 2013a. Monumentos de Sintra encerrados devido a queda de 2 mil árvores. ⟨http://expresso.sapo.pt/⟩ (last access: 29.12.13) (in Portuguese).

Expresso, January 21, 2013b. Temporal fecha Jardim Botânico de Coimbra. ⟨http://expresso.sapo.pt/⟩ (last access: 29.12.13) (in Portuguese).

Fink, A.H., Brücher, T., Ermert, V., Krüger, A., Pinto, J.G., 2009. The European storm Kyrill in January 2007: synoptic evolution, meteorological impacts and some considerations with respect to climate change. Nat. Hazards Earth Syst. Sci. 9, 405–423. http://dx.doi.org/10.5194/nhess-9-405-2009.

Fink, A.H., Pohle, S., Pinto, J.G., Knippertz, P., 2012. Diagnosing the influence of diabatic processes on the explosive deepening of extratropical cyclones over the North Atlantic. Geophys. Res. Lett. 39, L07803. http://dx.doi.org/10.1029/2012GL051025.

Freitas, J.G., and Dias, J.A., 2013. 1941 windstorm effects on the Portuguese Coast. What lessons for the future? In: Conley, D.C., Masselink, G., Russell, P.E. and O'Hare, T.J. (Eds.), Proceedings of the 12th International Coastal Symposium, Plymouth, England, Journal of Coastal Research, (Special issue no. 65), pp. 714–719, issn:0749-0208.

Haylock, M.R., Hofstra, N., Klein Tank, A.M.G., Klok, E.J., Jones, P.D., New, M., 2008. A European daily high-resolution gridded dataset of surface temperature and precipitation. J. Geophys. Res. (Atmospheres) 113, D20119. http://dx.doi.org/10.1029/2008JD10201.

Hodges, K.I., Lee, R.W., Bengtsson, L., 2011. A Comparison of extratropical cyclones in recent reanalyses ERA-Interim, NASA MERRA, NCEP CFSR, and JRA-25. J. Climate 24, 4888–4906. http://dx.doi.org/10.1175/2011JCLI4097.1.

Hoskins, B., McIntyre, M.E., Robertson, A.W., 1985. On the use and significance of isentropic potential vorticity maps. Q. J. R. Meteorol. Soc. 111, 877–946.

IPMA, Janeiro de 2013. Boletim Climatológico Mensal—IPMA January 2013 Monthly Climatology Report, IPMA, Lisboa (in Portuguese).

Klein Tank, A.M.G., et al., 2002. Daily dataset of 20th-century surface air temperature and precipitation series for the European Climate Assessment. Int. J. Climatol. 22, 1441–1453.

Knippertz, P., Wernli, H., 2010. A lagrangian climatology of tropical moisture exports to the Northern Hemispheric extratropics. J. Climate 23, 987–1003.

Lavers, D.A., Allan, R.P., Wood, E.F., Villarini, G., Brayshaw, D.J., Wade, A.J., 2011. Winter floods in Britain are connected to atmospheric rivers. Geophys. Res. Lett. 38, L23803. http://dx.doi.org/10.1029/2011GL049783.

Liberato, M.R.L., Pinto, J.G., Trigo, I.F., Trigo, R.M., 2011. Klaus—an exceptional winter storm over Northern Iberia and Southern France. Weather 66, 330–334. http://dx.doi.org/10.1002/wea.755.

Liberato, M.L.R., Pinto, J.G., Trigo, R.M., Ludwig, P., Ordóñez, P., Yuen, D., Trigo, I.F., 2013. Explosive development of winter storm Xynthia over the subtropical North Atlantic Ocean. Nat. Hazards Earth Syst. Sci. 13, 2239–2251. http://dx.doi.org/10.5194/nhess-13-2239-2013.

Liberato, M.L.R., Ramos, A.M., Trigo, R.M., Trigo, I.F., Durán-Quesada, A.M., Nieto, R., Gimeno, L., 2012. Moisture sources and large-scale dynamics associated with a flash flood event. In: Lin, J., Brunner, D., Gerbig, C., Stohl, A., Luhar, A., Webley, P. (Eds.), Lagrangian Modeling of the Atmosphere. American Geophysical Union, Washington, DC, http://dx.doi.org/10.1029/2012GM001244.

Ludwig, P., Pinto, J.G., Reyers, M., Gray, S.L., 2013. The role of anomalous SST and surface fluxes over the southeastern North Atlantic in the explosive development of windstorm Xynthia. Q. J. R. Meteorol. Soc. , http://dx.doi.org/10.1002/qj.2253.

Martius, O., Schwierz, C., Davies, H.C., 2007. Breaking waves at the tropopause in the wintertime northern hemisphere: climatological analyses of the orientation and the theoretical LC1/2 classification. J. Atmos. Sci. 64, 2576–2592. http://dx.doi.org/10.1175/JAS3977.1.

Muir-Wood, R., 2011. The 1941 February 15th Windstorm in the Iberian Peninsula. Trébol 56, 4–13.

Neu, U., Akperov, M.G., Bellenbaum, N., Benestad, R., Blender, R., Caballero, R., Cocozza, A., Dacre, H.F., Feng, Y., Fraedrich, K., Grieger, J., Gulev, S., Hanley, J., Hewson, T., Inatsu, M., Keay, K., Kew, S.F., Kindem, I., Leckebusch, G.C., Liberato, M.L.R., Lionello, P., Mokhov, I.I., Pinto, J.G., Raible, C.C., Reale, M., Rudeva, I., Schuster, M., Simmonds, I., Sinclair, M., Sprenger, M., Tilinina, N.D., Trigo, I.F., Ulbrich, S., Ulbrich, U., Wang, X.L., Wernli, H., 2013. IMILAST—a community effort to intercompare extratropical cyclone detection and tracking algorithms. Bull. Am. Meteor. Soc. 94 (4), 529–547. http://dx.doi.org/10.1175/BAMS-D-11-00154.1.

Newell, R.E., Newell, N.E., Zhu, Y., Scott, C., 1992. Tropospheric rivers?—A pilot study. Geophys. Res. Lett. 19 (24), 2401–2404. http://dx.doi.org/10.1029/92GL02916.

Peixoto, J.P., Oort, A.H., 1992. Physics of Climate. Am. Inst. of Phys., New York (520 pp).

Pinto, J.G., Reyers, M., Ulbrich, U., 2011. The variable link between PNA and NAO in observations and in multi-century CGCM simulations. Clim. Dyn. 36, 337–354. http://dx.doi.org/10.1007/s00382-010-0770-x.

Pinto, J.G., Zacharias, S., Fink, A.H., Leckebusch, G.C., Ulbrich, U., 2009. Factors contributing to the development of extreme North Atlantic cyclones and their relationship with the NAO. Clim. Dyn. 32, 711–737.

Portal da Marinha, January 19, 2013a. Salvamento de tripulantes do navio mercante "merle" após encalhe. ⟨http://www.marinha.pt/⟩ (last access: 23.4.14) (in Portuguese).

Portal da Marinha, January 21, 2013b. Registadas ondas de 19 metros durante o temporal do fim de semana. ⟨http://www.marinha.pt/⟩ (last access: 23.4.14) (in Portuguese).

Público, March 22, 2013a. Estado não pode lavar as mãos" da Mata Nacional do Buçaco. ⟨http://www.publico.pt/⟩ (last access: 29.12.13) (in Portuguese).

Público, February 19, 2013b. Temporal de Janeiro causou 30 milhões de euros de prejuízos. ⟨http://www.publico.pt/⟩ (last access: 29.12.13) (in Portuguese).

Público, March 26, 2013c. Cargueiro que estava encalhado na Murtosa já foi retirado. ⟨http://www.publico.pt/⟩ (last access: 23.4.14) (in Portuguese).

Raible, C.C., Della-Marta, P.M., Schwierz, C., Wernli, H., Blender, R., 2008. Northern hemisphere extratropical cyclones: a comparison of detection and tracking methods and different reanalyses. Mon. Weather Rev. 136, 880–897.

Ralph, F.M., Dettinger, M.D., 2011. Storms, floods, and the science of atmospheric rivers. Eos Trans. Am. Geophys. Union 92 (32), 265. http://dx.doi.org/10.1029/2011EO320001.

Ralph, F.M., Neiman, P.J., Wick, G.A., 2004. Satellite and CALJET aircraft observations of atmospheric rivers over the eastern North Pacific Ocean during the winter of 1997/98. Mon. Weather Rev. 132 (7), 1721–1745. http://dx.doi.org/10.1175/1520-0493(2004)132<1721:SACAOO>2.0.CO;2.

Ralph, F.M., Neiman, P.J., Wick, G.A., Gutman, S.I., Dettinger, M.D., Cayan, D.R., White, A.B., 2006. Flooding on California's Russian River: role of atmospheric rivers. Geophys. Res. Lett. 33, L13801. http://dx.doi.org/10.1029/2006GL026689.

Sanders, F., 1986. Explosive cyclogenesis in the West-Central North Atlantic Ocean, 1981–84. Part I: composite structure and mean behavior. Mon. Weather Rev. 114, 1781–1794.

Sanders, F., Gyakum, J.R., 1980. Synoptic-dynamic climatology of the "bomb". Mon. Weather Rev. 108, 1589–1606.

Schmith, T., Kaas, E., Li, T.-S., 1998. Northeast Atlantic winter storminess 1875–1995 reanaysed. Clim. Dyn. 14, 529–536.

Schneidereit, A., Blender, R., Fraedrich, K., Lunkeit, F., 2007. Icelandic climate and north Atlantic cyclones in ERA-40 reanalyses. Meteorol. Z. 16, 17–23.

Sickmöller, M., Blender, R., Fraedrich, K., 2000. Observed winter cyclone tracks in the northern hemisphere in re-analysed ECMWF data. Q. J. R. Meteorol. Soc. 126, 591–620.

Stohl, A., James, P., 2004. A Lagrangian analysis of the atmospheric branch of the global water cycle. Part 1: Method description, validation, and demonstration for the August 2002 flooding in central Europe. J. Hydrometeorol. 5, 656–678.

Stohl, A., James, P., 2005. A Lagrangian analysis of the atmospheric branch of the global water cycle. Part 2: Earth's river catchments, ocean basins, and moisture transports between them. J. Hydrometeorol. 6, 961–984.

Stohl, A., Forster, C., Sodemann, H., 2008. Remote sources of water vapor forming precipitation on the Norwegian west coast at 60°N – a tale of hurricanes and an atmospheric river. J. Geophys. Res. 113, D05102 〈10.1029/2007JD009006〉.

Trigo, I.F., Davies, T.D., Bigg, G.R., 1999. Objective climatology of cyclones in the Mediterranean Region. J. Clim. 12, 1685–1696.

Trigo, I.F., 2006. Climatology and interannual variability of Storm-Tracks in the Euro–Atlantic sector: a comparison between ERA-40 and NCEP/NCAR Reanalyses. Clim. Dynam. 26, 127–143.

Uccellini, L.W., Johnson, D.R., 1979. The coupling of upper and lower tropospheric jet streaks and implications for the development of severe convective storms. Mon. Weather Rev. 107, 682–703.

Ulbrich, U., Christoph, M., 1999. A shift of the NAO and increasing storm track activity over Europe due to anthropogenic greenhouse gas forcing. Clim. Dyn. 15, 551–559.

Ulbrich, U., Leckebusch, G.C., Pinto, J.G., 2009. Extra-tropical cyclones in the present and future climate: a review. Theor. Appl. Climatol. 96, 117–131.

Ulbrich, U., Leckebusch, G.C., Grieger, J., Schuster, M., Akperov, M., Yu., M., Bardin, Y., Feng, S., Gulev, M., Inatsu, K., Keay, S.F., Kew, M.L.R., Liberato, P., Lionello, I.I., Mokhov, U., Neu, J.G., Pinto, C.C., Raible, M., Reale, I., Rudeva, I., Simmonds, N.D., Tilinina, I.F., Trigo, S., Ulbrich, X.L., Wang, H., Wernli, The IMILAST team, 2013. Are greenhouse gas signals of northern hemisphere winter extra-tropical cyclone activity dependent on the identification and tracking methodology? Meteorol. Z. 22 (1), 61–68. http://dx.doi.org/10.1127/0941-2948/2013/0420.

Vilibic, I., Sepic, J., 2010. Long-term variability and trends of sea level storminess and extremes in European Seas. Global Planet Change 71, 1–12.

Wang, X., Feng, Y., Compo, G.P., Swail, V.R., Zwiers, F.W., Allan, R.J., Sardeshmukh, P.D., 2012. Trends and low frequency variability of extra-tropical cyclone activity in the ensemble of twentieth century reanalysis. Climate Dyn., 1–26. http://dx.doi.org/10.1007/s00382-012-1450-9.

Wang, X.L.L., Swail, V.R., Zwiers, F.W., 2006. Climatology and changes of extra-tropical cyclone activity: Comparison of ERA-40 with NCEP-NCAR reanalysis for 1958–2001. J. Climate 19, 3145–3166.

Wernli, H., Dirren, S., Liniger, M.A., Zillig, M., 2002. Dynamical aspects of the lifecycle of the winter storm 'Lothar' (24–26 December 1999. Q. J. R. Meteorol. Soc. 128, 405–429.

Wernli, Heini, Sprenger, Michael, 2007. Identification and ERA-15 Climatology of Potential Vorticity Streamers and Cutoffs near the Extratropical Tropopause. J. Atmos. Sci. 64, 1569–1586. http://dx.doi.org/10.1175/JAS3912.1.

Zhu, Y., Newell, R.E., 1998. A proposed algorithm for moisture fluxes from atmospheric rivers. Mon. Weather Rev. 126 (3), 725–735. http://dx.doi.org/10.1175/1520-0493(1998)126<0725:APAFMF>2.0.CO;2.